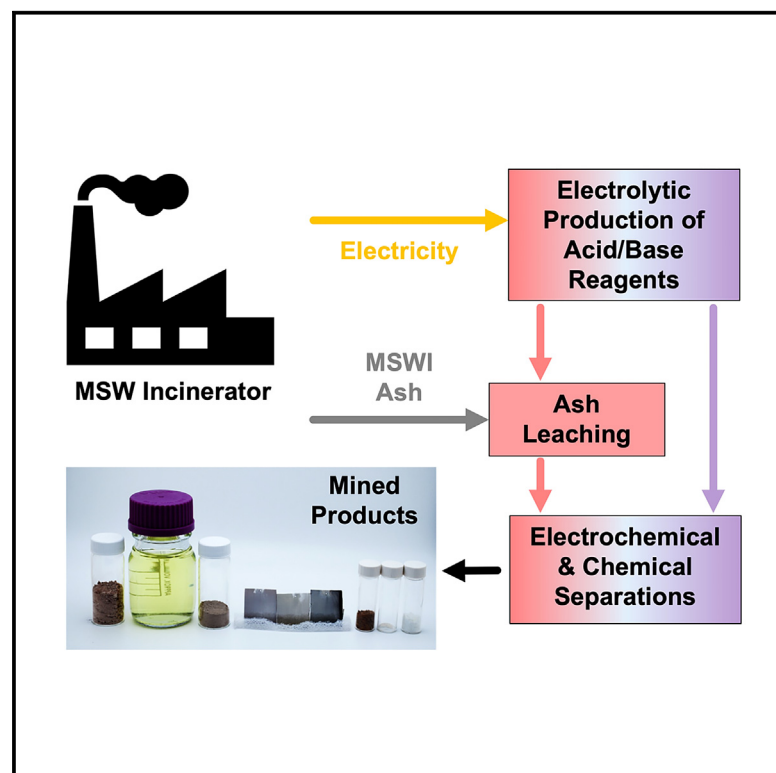


# Toward zero-waste resource recovery from municipal solid waste incineration ash by electrochemical and chemical mining

## Graphical abstract



## Authors

Duhan Zhang, Michael J. Wang, Sophie C. Coppieters 't Wallant, Sonia Zhang, Yet-Ming Chiang

## Correspondence

ychiang@mit.edu

## In brief

Municipal solid waste incineration (MSWI) is a crucial process for electricity generation and global landfill reduction. MSWI ash, considered a negative-value waste stream, represents an untapped resource as a feedstock for urban mining. Our work develops a process for separating ash into valuable product streams without additional waste using electrochemical and chemical methods, which can be extended to other waste streams. The technoeconomical model demonstrates its economic feasibility and scalability.

## Highlights

- Proposed a route for mining MSWI ash using electrolytically produced reagents
- Experimentally demonstrated recovery of eight target compounds from the MSWI ash
- Conducted technoeconomic analysis showing positive returns for the ash mining process

## Article

# Toward zero-waste resource recovery from municipal solid waste incineration ash by electrochemical and chemical mining

Duhan Zhang,<sup>1,2</sup> Michael J. Wang,<sup>1,2</sup> Sophie C. Coppieters 't Wallant,<sup>1</sup> Sonia Zhang,<sup>1</sup> and Yet-Ming Chiang<sup>1,3,\*</sup>

<sup>1</sup>Massachusetts Institute of Technology, Department of Materials Science and Engineering, Cambridge, MA 02139, USA

<sup>2</sup>These authors contributed equally

<sup>3</sup>Lead contact

\*Correspondence: [ychiang@mit.edu](mailto:ychiang@mit.edu)

<https://doi.org/10.1016/j.crsus.2024.100120>

**SCIENCE FOR SOCIETY** Municipal solid waste incineration (MSWI) is an important part of our waste and energy landscape. Aside from generating useful electricity, the MSWI process also helps to control the size of our landfills, which represent the third largest source of anthropogenic methane emissions. However, due to the proliferation of cheap wind and solar energy in the US, it is becoming increasingly difficult for MSWI facilities to generate net positive cash flows from electricity sales due to the high costs of disposal of the MSWI byproduct ash. Against this backdrop, we recognize that MSWI ash contains a plethora of valuable compounds that raise the following question: can sufficient value be extracted from the MSWI ash to “beat electricity” as a product? In this work, we investigate processes for mining MSWI ashes that are powered by MSWI electricity to extract valuable ash-derived products, which ultimately results in technoeconomic returns greater than the sale of the electricity itself.

## SUMMARY

Municipal solid waste incineration (MSWI) plays a critical role in our waste and energy ecosystem by reducing waste volume and generating electricity. However, the economic viability of MSW incinerators is at risk due to declining electricity prices. Meanwhile, MSWI ash represents an untapped resource for valuable compounds, with an embodied value of \$100–\$400/tonne, contrasted with incurred landfilling expenses (~\$50/tonne). Here, we propose an integrated process utilizing MSWI electricity to power electrochemical and chemical processes for mining MSWI ash. We demonstrate a sequential process of leaching, electrowinning, and hydroxide precipitation, utilizing electrolytically produced reagents, to recover elements from the ash with purified silica as a co-product. We demonstrate >90% recovery of target elements, with purities >90% for most elements. Additionally, our technoeconomic analyses suggest that the net economic returns are double those of current MSWI practices based on the sale of electricity. The proposed process can be extended to waste streams beyond MSWI ash.

## INTRODUCTION

The disposal of municipal solid waste (MSW) is a growing environmental and societal concern that is increasingly aggravated by global urbanization. In the United States, over 150 million tonnes of MSW (50%) are added to landfills annually,<sup>1</sup> releasing an estimated 103 million tonnes of CO<sub>2</sub> equivalent in 2021 from the decomposition of organic MSW into methane.<sup>2,3</sup> This represents the third largest (14.3%) source of anthropogenic methane emissions in the United States. Although the majority of MSW in the United States goes directly into landfills, 13% of MSW is incinerated at waste-to-energy (WTE) facilities, producing 14

billion kWh of electricity (past decade average) and 6.6 million tonnes of ash in the United States (in 2020) and reducing the corresponding domestic landfill volume by 95%–85% and mass by 85%–75%.<sup>4–7</sup>

Because WTE facilities rely on electricity sales for revenue, declining electricity prices are putting WTE facilities at risk, which may lead to substantial increases in MSW landfill sizes and methane emissions in the future. Against this backdrop, the ash byproduct of MSW incineration (MSWI) represents an untapped resource for valuable materials, originating predominantly from consumer products, the production of which has already incurred environmental and economic costs. The metals

contained in MSW globally are valued at up to \$50 billion annually, mostly in the form of e-waste.<sup>8,9</sup> However, aside from ferrous/non-ferrous metals recovery, the majority of MSWI ash is currently landfilled at a negative value due to the tipping fees charged for ash disposal.<sup>10</sup> Thus, recovery of technology-critical materials from this waste stream represents a potential positive-value alternative to ash disposal and an opportunity to contribute to a circular materials economy.<sup>11,12</sup> This work investigates the technical and economic viability of such a scheme.

Compared with other waste streams, MSWI ash is composed of a plethora of elements spanning the periodic table, with concentrations ranging from parts per billion (ppb) to several percent (Figure 1A).<sup>13–18</sup> Several approaches in literature have proposed strategies for recovering materials from various waste streams with varying degrees of efficiency and selectivity, including selective leaching,<sup>19–21</sup> electrowinning,<sup>22</sup> pH-swing precipitation,<sup>21</sup> and solvent extraction.<sup>23</sup> Although many of these methods have been able to successfully recover key critical materials out of specific waste streams, for example, copper from e-waste, these processes typically only target the recovery of one element. This can result in poor technoeconomic viability and the creation of additional waste streams. Aside from materials recovery, others have proposed utilizing ash in asphalt and concrete applications.<sup>4,17,24</sup> Although this reduces the need to landfill the ash and offsets greenhouse gas emissions by offsetting cement demand, this application does not allow for the reuse of critical materials embedded in the ash.

An ideal process for mining MSWI ash should offer the flexibility to selectively recover many elements such that the ash can be completely separated into valuable product streams without additional waste streams being created. Here, we propose an electrochemically based process in which WTE electricity powers an electrolyzer that produces acid and base reagents for subsequent processing. This approach is inspired by work by Ellis et al.<sup>25</sup> in which electrolytically produced acid and base were used for processing decarbonized cement. We demonstrate proof-of-concept experiments utilizing electrolytically produced reagents for the leaching of metals from ash and subsequent sequential recovery of leached metals through a combination of electrowinning and pH-mediated precipitation of metal hydroxides. We show that the proposed mining operation can be powered entirely by WTE electricity, requiring only salt, water, and electricity as inputs (Figures 1B and 1C), without the creation of additional waste streams. A first-order technoeconomic analysis of the integrated process shows that the net revenue from the mining of a representative ash (~\$120/tonne) is about twice the revenue from WTE electricity sales (~\$55/tonne). The results show that WTE electricity-powered electrochemical mining could be a viable materials recovery strategy and provide a generalized framework for resource recovery that can be expanded to waste streams beyond MSWI ash.

## RESULTS AND DISCUSSION

### MSWI mining concept and recovery strategy

MSWI ashes can contain over 60 elements in concentrations ranging over eight orders of magnitude, making the selectivity and yield of recovering target elements the determining factors

for a viable MSWI mining technology.<sup>14,15</sup> Aqueous electrochemical processes have inherent advantages for selectivity in the sense that both system potential and pH can be finely controlled with externally applied voltages. An example of such a process was previously demonstrated for ambient temperature production of cement.<sup>25</sup> In this process, salt electrolysis was used to simultaneously produce the necessary acidic conditions to extract Ca from limestone and the alkaline conditions necessary to selectively precipitate hydrated lime. Extending upon this idea, the following process proposes a similar methodology relying on electrolytically produced acids and bases for extracting elements out of MSWI ash and recovering them as valuable products.

The proposed process begins with the extraction of target elements from MSWI ash by leaching in an electrolytically produced acid. Salt electrolysis for acid and base production is a highly scaled technology, with technologies like electrolyzers and electrodialysis with bipolar membranes playing major roles in the chemicals, food, and water treatment industries.<sup>26,27</sup> The most prominent example is the chlor-alkali process, which, in combination with an acid burner, produces hydrochloric acid (HCl) and NaOH solution from the electrolysis of NaCl.<sup>26,27</sup> Herein, we use HCl as our model acid for leaching target metals from the ash.

Once speciated, a subset of elements can be recovered in metallic form by electrowinning from the leachate. Theoretical values of the electrowinning potential (Equations S1 and S2) for various metals of interest are listed in Table S1. Those elements that cannot be electrowon can be recovered by metal hydroxide precipitation. Theoretical values of the pH above which metal hydroxide precipitation will occur are also listed in Table S1, based on tabulated solubility products,  $K_{sp}$  (Equations S3 and S4). For NaCl electrolysis, HCl and NaOH are produced in equimolar quantities and can be used for these purposes.

In order to most efficiently recover the maximum number of elements, an order of operations based on the graphical representation of the electrowinning potentials and hydroxide precipitation pH values for 42 elements in Figure 2A is proposed. For most metals, the metallic form has a greater market value than the metal salt; hence, electrowinning is preferred where possible. Starting with acidic leachate, for maximum separation, metals should be recovered in order of increasingly negative reduction potentials (starting at the far right in Figure 2A) because all metals with a higher reduction potential than the applied potential will be simultaneously electrowon. For aqueous electrolytes, the reduction of metal cations at low potentials is generally limited by the hydrogen evolution reaction (HER), the onset of which decreases Faradaic efficiency and raises electrolyte pH. The HER potentials for various pH values are shown as horizontal lines in Figure 2A. Although there have been examples of aqueous electrowinning of metals far below the HER potential,<sup>28–30</sup> for illustration, we limited electrowinning to metals with reduction potentials equal to and above that of Zn. Hydroxide precipitation may then be conducted for elements of lower reduction potential (left half of Figure 2A). Similarly, for selective separation, metal hydroxides should be precipitated in order of increasing pH. (Similar considerations

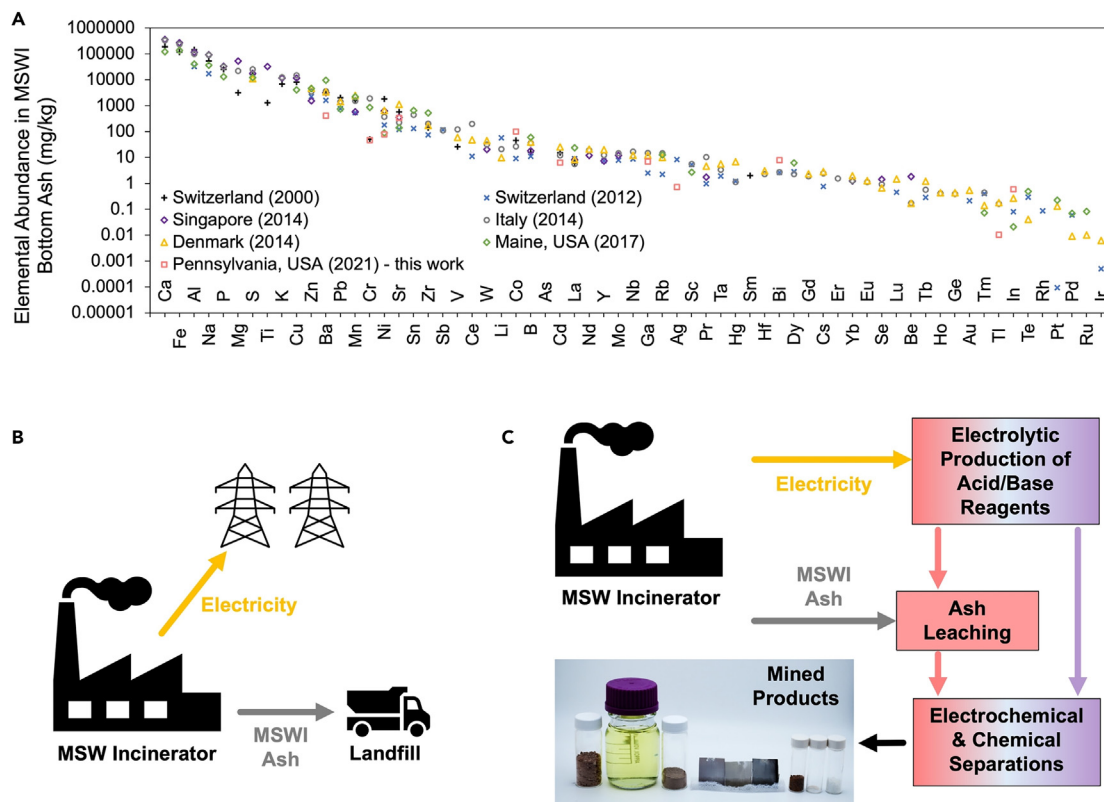


**Figure 1. Elemental abundance in representative MSWI ashes and current and proposed modes of operation for MSW incinerators**

(A) Elements and their concentration in MSWI bottom ash ranked by their average abundance.

(B) Current scheme of MSW incinerators, which profit from electricity sales and incur disposal fees for ash landfilling.

(C) Proposed mining operation utilizing electricity and ash to power electrochemical and chemical processes for recovering<sup>3,4</sup> materials from MSWI ash.

apply for precipitation of any metal salt, e.g., carbonates or oxalates, from the leachate.)

In summary, our proposed recovery strategy follows the sequential process: (1) ash leaching in acidic solution, (2) sequential electrowinning of metals at increasingly negative potentials, and (3) sequential precipitation of hydroxides at increasing solution pH. Although complete separation of all elements in the ash can be achieved in theory through these two methods, economic viability will ultimately depend on the elemental concentrations in the ash and the elemental value embedded in the ash.

### Analysis of mineral value embodied within MSWI ash

Assuming that all of the elements in MSWI ash could be separated into their individual components, a hypothetical mineral value of the ash can be assigned. The value of each individual element can be quantified based on the product of its concentration in the ash (kg/tonne) and the commodity price of the element in its recoverable form (\$/kg), either a metal or metal hydroxide. The commodity prices of elements along with assumptions surrounding those prices are listed and described in Table S2. It is assumed that all metals with a reduction potential within the stability limits of aqueous solutions can be electrowon, while all other elements can be

precipitated as hydroxides. Accordingly, the total mineral value of the ash is the sum of the values of all its individual components:

$$\text{Ash Value} \left( \frac{\$}{\text{mton}} \right) = \sum_{M = \text{element}} \text{Concentration of Element} \times M \left( \frac{\text{kg}}{\text{mton}} \right) \times \text{Value of Element } M \left( \frac{\$}{\text{kg}} \right) \quad (\text{Equation 1})$$

The cumulative values for several MSWI ashes are plotted as a function of the elements, listed in order of increasing value in the ash (Figure 2B). Based on ash compositions in literature, the mineral value of these MSWI ashes ranges from \$100/tonne to \$400/tonne. These calculated ash values are likely underestimated since none of the datasets report concentrations for all 66 elements listed. Taking the concentration of each element in Figure 2B to be the average of its concentration in the seven different ashes and summing the value across all 66 elements, we arrive at a potentially recoverable MSWI ash value of \$340/tonne. This value far exceeds the average US selling price of large commodity materials such as ordinary Portland cement (\$130/tonne<sup>31</sup>) and recycled glass cullet (\$100/tonne<sup>32</sup>). In addition, complete utilization of the ash would avoid an average landfilling fee in the US of ~\$50/tonne.<sup>33</sup>

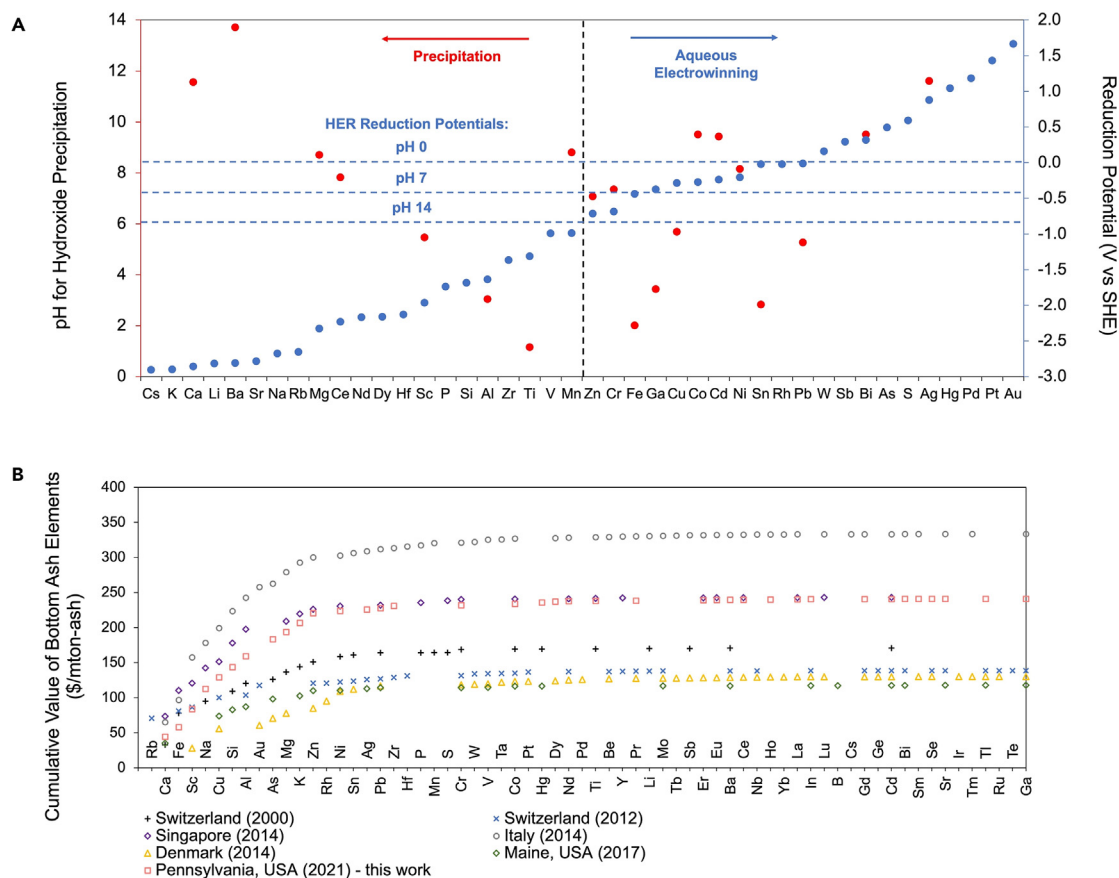


**Figure 2. Element separation strategy and cumulative elemental values for representative bottom ashes**

(A) The calculated reduction potentials for various elements in MSWI ash (right) and the calculated pHs for hydroxide precipitation (left). The HER potentials are shown at various pHs. Below the HER potential, HER is favorable, and thus electrowinning metals far below the HER potential is challenging due to low Faradaic efficiency and unstable increases in electrolyte pH. Thus, the metals amenable to aqueous electrowinning include all elements to the right of the plot beginning with Zn, while the elements to the left are amenable to recovery by hydroxide precipitation. The pHs for hydroxide precipitations are based on the hydroxide precipitation from an increase in pH as opposed to a decrease in pH from solubilized amphoteric metals.

(B) Cumulative value of bottom ash elements, calculated based on the concentration and the value of each element. The elements are ranked from left to right based on the average fractional value in the ash.

However, the majority of the ash value is represented by only a few elements, with 90% of the ash value being represented by the first 15 elements, which each contribute between ~3%–15% of the total ash value (Figure 2B). Of these 15 elements, nine (Ca, Fe, Na, Cu, Si, Al, Mg, K, and Zn) are among the most abundant elements found in MSWI ash generally, existing in concentrations between 3,000 mg/kg to 15 wt %. Although MSW widely varies in composition, both geographically and temporally, the average value of these nine elements within the seven ashes shown in Figure 1A is \$129/tonne, with a standard deviation of \$56/tonne. The other six (Rb, Sc, Au, As, Rh, and Ni) are highly valuable but only present in low concentrations, between 5 and 500 mg/kg. Scandium, for example, is present at very low concentrations (<10 mg/kg) but represents up to 21% of the total ash value. The remaining ~50 elements comprise about 10% of the ash value and include critical elements, such as Nd, but their low abundance and value suggest that cost-effective recovery is unlikely.

### Proposed process flow

Based on the combination of elemental value (Figure 2B) and technical feasibility for recovery (Figure 2A), eight target elements representing ~\$123/tonne value were targeted for recovery: Cu, Pb, Zn, Al, Fe, Mg, Ca, and Si. Sodium is excluded from this list because it is not recovered, being fully dissolved as NaCl or NaOH throughout the process. A proposed process, Figure 3, begins with a chlor-alkali reactor, co-located with and powered by the WTE facility, from which a stream of HCl is produced for ash leaching. The acid-leaching step solubilizes the majority of metals, leaving behind a SiO<sub>2</sub>-rich residue, which is utilized as discussed later. Next, Cu, Pb, and Zn are selectively electrowon in metallic form from the leachate at −0.3, −0.5, and −1.0 V vs. standard hydrogen electrode (SHE), respectively, also using WTE electricity. Following electrowinning, NaOH co-produced by the chlor-alkali electrolyzer is used to increase the pH of the remaining leachate and sequentially precipitate Al, Fe, Mg, and Ca as hydroxides at pHs 9, 11, and 14, respectively. Finally, the acid and alkaline waste



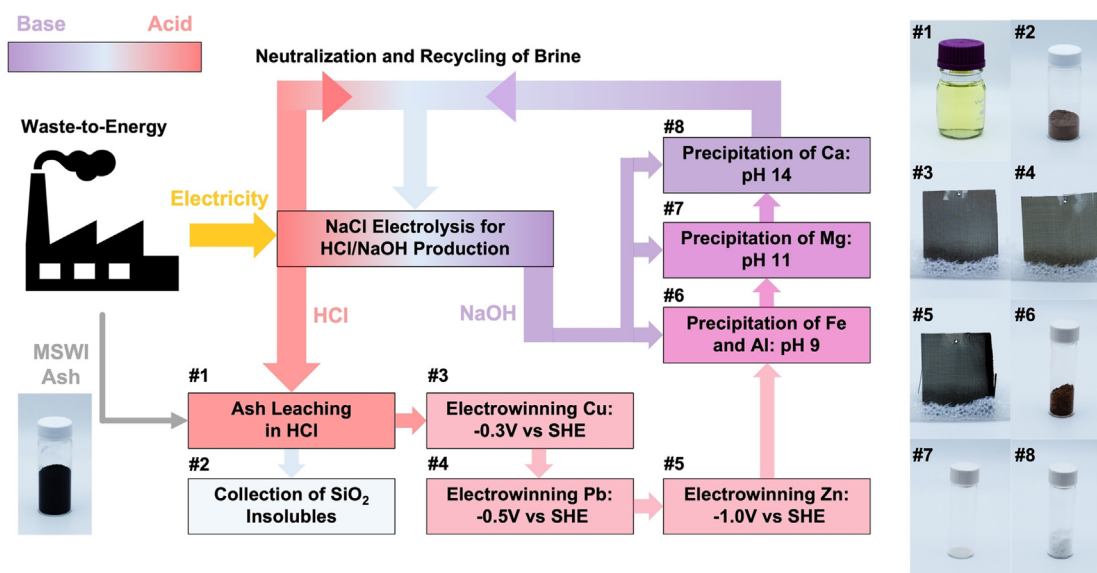


**Figure 3. Zero-waste electrochemically based process for mining MSWI ash based on present experimental findings**

Photographs show the input and output materials resulting from a lab-scale execution of the proposed process. The number of each photo corresponds to a given step in the process diagram on the left.

streams are recombined, forming a neutralized NaCl brine that is recirculated into the chlor-alkali electrolyzer. This proposed process can separate MSWI ash into multiple product streams, operate solely on water, NaCl (or other salts), and WTE electricity, and generate no additional waste streams except for excess salt, which may accumulate in the brine over time. In the following sections, we present proof-of-concept experiments from which the efficacy and technoeconomics of leaching, electrowinning, and precipitation are evaluated.

### Representative MSWI ash for the experimental study

For experimentation, an MSWI bottom ash sourced from a WTE facility in York County, Pennsylvania was selected. This ash has

a value of \$120/tonne for the eight target elements, near the average value in Figure 2B. After leaching of the MSWI ash in 1, 2, and 5 M HCl for 24 h at room temperature, the primary constituents of the ash leachate are Ca, Al, Fe, Mg, and Na (Table 1). For about half of the elements, systematically higher leachate concentrations were observed with increasing HCl concentrations, while others showed no clear trend, potentially due to sample-to-sample variations in the ash. All leachate concentrations were considered to be sufficiently high for the experiments discussed below. However, for technoeconomic reasons discussed later, the 1 M leachate was used in the subsequent experiments.

X-ray diffraction (XRD) was conducted on the as-received ash and compared with results for the acid-insoluble material collected after acid leaching (Figures 4A–4C). The X-ray diffractogram, Figure 4C, shows that the crystalline components of the as-received ash are primarily quartz ( $\text{SiO}_2$ ) and calcite ( $\text{CaCO}_3$ ). An expanded view, Figure S1, shows that the starting ash also has minor amounts of the crystalline phases halite ( $\text{NaCl}$ ), magnesioferrite ( $\text{MgFe}_2\text{O}_4$ ), iron oxide ( $\text{Fe}_2\text{O}_3$ ), and gypsum ( $\text{CaSO}_4$ ). The acid-insoluble residue, on the other hand, is composed of quartz as the primary crystalline phase along with small amounts of residual crystalline phases. Also detectable is a broad background indicating an amorphous phase, a majority of which is most likely carbon, since the incinerator that produces this particular MSWI ash operates in an oxygen-lean environment according to the WTE operators, leading to ~20 wt % carbon in the ash. Amorphous silica may also comprise some of this non-crystalline material. Rietveld refinement of the diffraction pattern indicated the presence of 80 wt % amorphous phase, 15 wt % quartz, and 5 wt % of a mixture of various (Ca, Mg, Fe, Al)  $\text{SiO}_x$  silicates and rutile  $\text{TiO}_2$ .

**Table 1. The concentration of elements in the MSWI ash leachates dissolved in 1, 2, and 5 M HCl for 24 h at room temperature, measured using ICP-OES**

All concentrations in units of mg/L							
	1 M	2 M	5 M		1 M	2 M	5 M
Al	2,346	5,992	7,000	B	13	36	67
Ca	7,950	9,920	12,223	Ba	2	4	5
Cu	50	282	334	Bi	3	2	3
Fe	1,851	5,074	7,719	Cd	1	4	54
K	222	598	448	Co	8	27	24
Mg	853	1,363	1,786	Cr	4	11	19
Na	1,125	1,349	1,044	Ga	9	14	10
Pb	65	93	399	Li	67	57	54
Zn	340	973	647	Mn	52	97	109
–	–	–	–	Ni	7	22	28
–	–	–	–	Sr	18	33	20

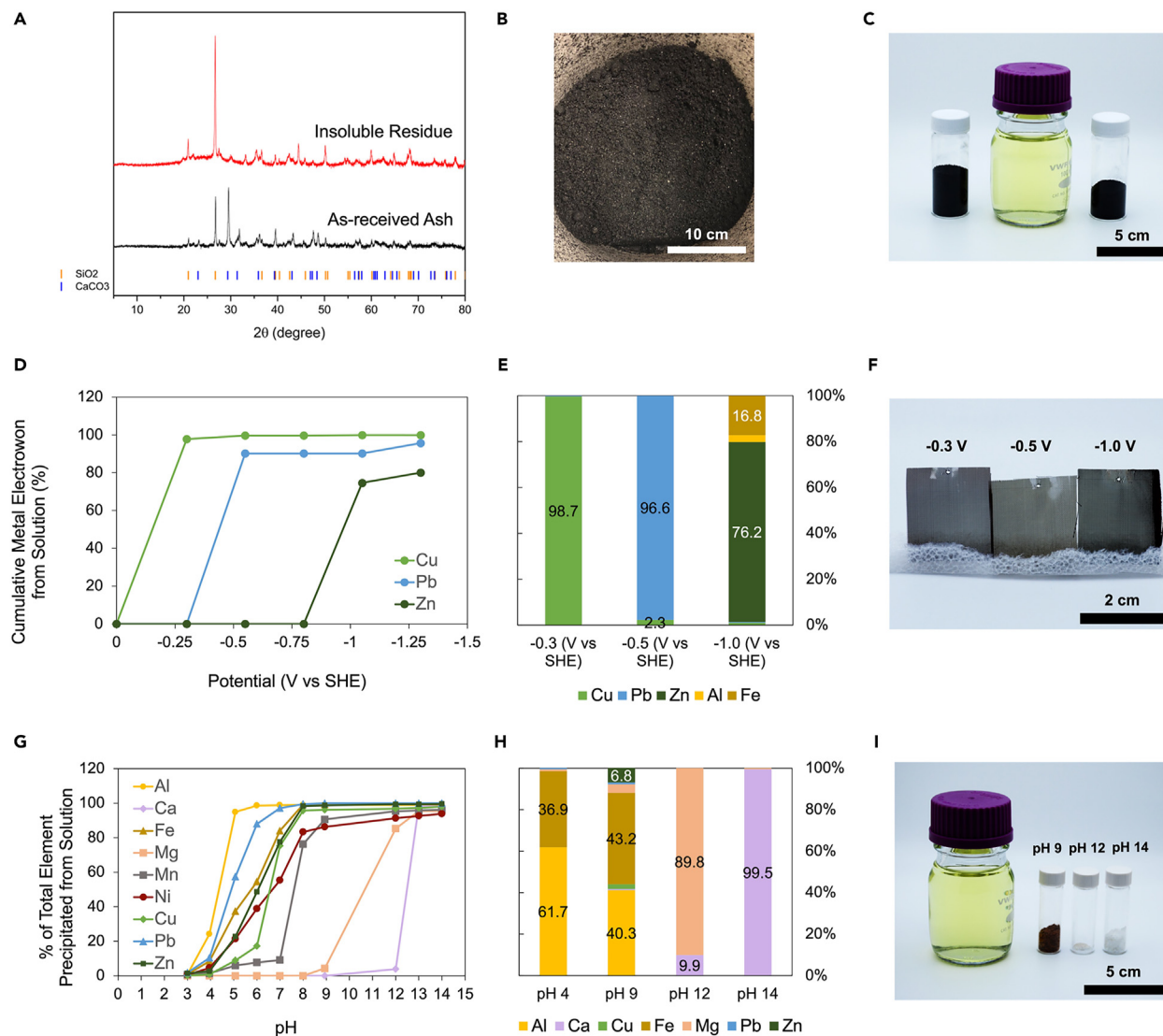


**Figure 4. Experimental findings illustrating proposed MSWI mining process**

First row: images of starting ash and acid-insoluble residue after leaching.

(A) X-ray diffraction spectra for the starting MSWI ash and the remaining insoluble residue after leaching in 1 M HCl and vacuum filtration.

(B) MSWI ash sourced from York County, PA, USA.

(C) From left to right: MSWI ash, the 1 M HCl leachate (based on a 0.1 solid-liquid ratio), and remaining insoluble material. Second row: recovery of metals via sequential electrowinning at decreasing potentials. Recovery of elements out of a 1 M HCl leachate at each sequential potential.

(D) The compositions of the collected electrode deposits at -0.3, -0.5, and -1.0 V (vs. SHE) as measured by ICP-OES.

(E) Photographs of the metal-coated electrodes after electrowinning at the designated potential. The electrode deposits consist mainly of Cu (-0.3 V), Pb (-0.5 V), and Zn (-1.0 V), with the detailed compositions shown in (D). Third row: recovery of metal hydroxides via sequential precipitation at increasing pH.

(G) Recovery of elements out of a 1 M HCl leachate at each sequential pH.

(H) The compositions of the collected precipitates at pH 4, 9, 12, and 14 as measured by ICP-OES.

(I) Photographs of the starting HCl leachate and the precipitates collected after precipitation at the designated pHs. The precipitates consist mainly of Al and Fe (pH 9), Mg (pH 12), and Ca (pH 14), with the detailed compositions shown in (H).

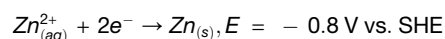
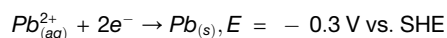
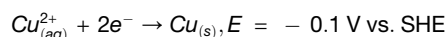
The acid-insoluble component of the ash was found to contain <0.1 wt % of toxic metals such as Cu, Cd, and Pb, compared with ~0.5 wt % in the starting ash, showing that the acid-leaching process has produced a more environmentally benign residue than untreated MSWI ash. As shown later, one of the electrowon metals is Pb. Such purified residue could

be landfilled with a lower risk of groundwater contamination than conventional ash, but would still constitute an additional waste stream that incurs disposal costs. Alternatively, this material could be used as a supplemental cementitious additive (SCM) in concrete.<sup>34–36</sup> XRD characterization and Rietveld refinement of the material using an internal Si standard show

that the remaining SiO<sub>2</sub> is primarily amorphous SiO<sub>2</sub> (70 wt %) with the remaining SiO<sub>2</sub> retaining a quartz structure. The combination of high silica content and low crystallinity suggests a high pozzolanic reactivity. Indeed, a standard test of the pozzolanic reactivity of the silica with calcium hydroxide,<sup>34</sup> based on thermogravimetric analysis of the reacted mixture (Figure S2), showed that the acid-insoluble material has similar pozzolanic reactivity to fly ash, a well-known SCM that typically sells for ~\$75/tonne<sup>37</sup> in the US. Thus, the leached MSWI ash constitutes an additional product stream, eliminates the need for landfill disposal, and avoids the landfill tipping fee (\$50/tonne). The additional revenue gains from this avoidance are included in the technoeconomic analysis. We do not, however, include the economic benefits of avoided pollution, which would be evident in a full life cycle analysis.

### Metals recovery by electrowinning

The efficacy of metals recovery by electrowinning from the ash leachate was evaluated through a series of potentiostatic experiments. Similar experimental configurations and strategies have been used to sequentially electrowin series of metals from waste leachates, such as e-waste.<sup>13,38–40</sup> Due to their relatively high concentrations and their relevance in commodity markets, the main metals of interest for electrowinning are Cu, Pb, and Zn. In HCl solution, the expected cathodic reactions for electrowinning of these metals at the given leachate concentrations are as follows:



Based on the expected reduction potentials, a sequential electrowinning experiment was conducted where a 1 M HCl leachate was subjected to a constant cathodic potential for 1 hr. After electrowinning at the constant potential, the leachate was subjected to another hold at a lower potential. Based on the reduction potentials, the metals should be won in order of Cu, Pb, and Zn. Because electrowinning kinetics are dependent upon the overpotential (the deviation from the equilibrium potential), five descending potential steps (−0.3, −0.5, −0.8, −1.0, −1.25 V vs. SHE) were chosen for evaluating the efficacy of electrowinning. Inductively coupled plasma (ICP) analysis of the leachate (3 mL) was conducted before and after each potentiostatic experiment and used to calculate the metal recovery percentage throughout the sequential process (Figure 4D). Additionally, after each electrowinning step, the electrode deposits were collected, rinsed with DI water, and then redissolved for compositional analysis using ICP (Figure 4E). After the first potential step at −0.3 V, 97% of the Cu was recovered from the solution, with no Pb and Zn recovered, as expected from the reduction potentials. Compositional analysis of the electrodeposits is in good agreement, showing a Cu purity of 98.7%, with the remaining balance composed of Bi, which is in trace concentrations in the leachate but has a higher reduction potential than Cu (0.2 V).

For the next step at −0.5 V, 90% of the Pb was recovered from the solution, and has a purity of 96.6% based on the compositional analysis. The remaining impurities are primarily Cu, which represents the 2.3% of the Cu that was not electrowon within the first step. This highlights the need for high recovery efficiencies to produce high-purity metals in a sequential process such as the experiment conducted here. Any metals not completely electrowon will be electrowon or precipitated as impurities in a later stage of the recovery process. Zn recovery did not begin to occur until −1.0 V, indicating a high overpotential required for electrowinning, and 75% was recovered after 1 h. Only an additional 5% of Zn was recovered after another 1 h at −1.25 V, a potential at which H<sub>2</sub> evolution (bubbling) was dominant.

The electrodeposits collected after the −1.0 V step is primarily Zn, at 76.2% concentration. However, the Zn contains significant amounts of Fe (16.8%) and Al (3%) impurities. The reduction of Fe<sup>2+</sup> to Fe<sup>0</sup> is expected to co-deposit with Zn at a potential of −1.0 V (vs. SHE); however, the deposition of Al<sup>0</sup> is not expected given its low reduction potential (−2 V vs. SHE). A fraction of the detected Fe and the Al impurities are therefore attributed to the precipitation of Fe(OH)<sub>3</sub> and Al(OH)<sub>3</sub> on the electrode surface due to local increases in pH caused by the significant hydrogen evolution. The challenge of removing Fe impurities from Zn electrodeposits has been a long-standing challenge for electrolytic Zn production and typically requires a pre-treatment of the leachate to separate Fe from Zn.<sup>41</sup> Based on these results, we show that within our proposed process flow, the recovery of Cu, Pb, and Zn at −0.3, −0.5, and −1.0 V (Figure 4F) provides the best balance between recovery efficiencies (>90% for Cu and Pb, >80% for Zn) and high selectivity (~99% purity for Cu, ~97% for Pb, ~76% for Zn), while leaving behind the remaining target elements for recovery by hydroxide precipitation. Although these experimental purities are relatively low (e.g., electrical grade copper is 99.95% pure), the technoeconomic analysis takes the observed purity into account (see Table S2 for further detail). Since the market price for most materials increases sharply as 100% purity is approached, there is a clear opportunity to further increase economic return by optimizing the current processes for purity. Naturally, further purification could also be conducted at the MSWI plant or by external refiners.

### Metal hydroxide recovery using pH swing-induced precipitation

The chlor-alkali process produces one unit of base along with each unit of acid produced. This stream of base can be used for selective precipitation of the remaining elements as metal hydroxides. The efficacy and selectivity of elemental recovery via precipitation were evaluated through a similar sequential process as was conducted for electrowinning (Figure 4G). Beginning with a 1 M (pH = 0) HCl leachate, the solution pH was sequentially increased by 1 pH unit through the addition of NaOH. After equilibration, any precipitated solids were filtered and separated from the remaining leachate. The pH of the remaining leachate was then increased stepwise, and this process was repeated until a final pH of 14. As expected from Figure 2A, the first elements to precipitate are Al and Fe at pH 3. Of the elements in solution, Al and Fe are the third and fourth most



**Table 2. Rare earth elements content in the starting ash and outputs of the mining operation**

REE concentrations in dry material (mg/kg)																	
–	Sc	Y	La	Ce	Pr	Nd	Sm	Eu	Gd	Dy	Ho	Er	Tm	Yb	Lu	Th	U
Starting ash	0.5	4.5	3.7	6.2	0.7	2.6	0.5	0.1	0.6	0.3	0.1	0.2	0	0.4	0	0.3	0.3
pH 9 precipitates	1.8	15.2	13	21.9	2.5	9.1	1.6	0.5	2.1	1.1	0.2	0.6	0.1	1.3	0.1	1	0.9
REE concentration factors	3.6	3.3	3.5	3.5	3.5	3.5	3.5	3.5	3.5	3.5	3.5	3.5	3.5	3.5	3.6	4	3.6

The concentrations are measured by ICP-MS.

abundant elements in the ash leachate. Although all the Al is precipitated by a pH of 4, the amount of Fe precipitated out of the solution gradually increases with increasing pH and is not completely precipitated until pH 7. It is hypothesized that this is due to the presence of multiple iron valence states with different solubility products (i.e.,  $\text{Fe}^{2+}$   $K_{\text{sp}} = 4.9 \times 10^{-17}$ ,  $\text{Fe}^{3+}$   $K_{\text{sp}} = 2.8 \times 10^{-39}$ ).<sup>42</sup> However, in the range of pH 3–7, a number of less abundant elements also precipitate, including Cu, Pb, Zn, Ni, and Mn. The elements that can be electrowon, such as Cu, Pb, and Zn, can be recovered prior to the precipitation process. At higher pHs, Mg is observed to precipitate nearly completely at pH 12, and Ca is observed to precipitate at pH 13. Since almost all other elements have precipitated out of the leachate by pH 12, the purities of the  $\text{Mg}(\text{OH})_2$  and  $\text{Ca}(\text{OH})_2$  are quite high (89.8% and 99.5%, respectively), Figure 4H. By pH 14, the only metals remaining in solution are the alkali metals (Li, Na, K).

The compositions of precipitates collected at pH 4, 9, 12, and 13 were measured by ICP optical emission spectroscopy (ICP-OES) analysis (Figure 4H). Of the known elements present in the ash leachate, Mg and Ca can be selectively and completely precipitated as a metal hydroxide. Al and Fe can be nearly completely precipitated as hydroxides but have not been separated from each other due to incomplete precipitation of Fe at lower pHs. Note that the relative concentrations of the mixed Al and Fe hydroxides recovered at pH 9 in Figure 4H are similar to their concentrations in the residue from bauxite refining for aluminum, referred to as “red mud.” Therefore, we find that pH-swing precipitation can recover a Fe/Al mixture, Mg, and Ca hydroxides at pHs 9, 12, and 13, respectively.

### PMs and rare earth content

Previous urban mining efforts have targeted the recovery of critical materials such as platinum group metals (PGMs), precious metals (PMs), and rare earth elements (REEs).<sup>13</sup> Using ICP mass spectrometry (ICP-MS) analysis, it was determined that the concentrations of Ru, Rh, Pd, Re, Os, Ir, Pt, and Au in the starting ash are each below 10  $\mu\text{g}/\text{kg}$ . Based on the value of these metals, the PGM value embodied in the ash is <\$2/tonne, which probably cannot justify the recovery costs.

Similarly, the REE content in the ash quantified by ICP-MS is  $\sim 20$  mg/kg, with the most abundant elements being Y, Ce, Nd, La, and Pr (Table 2). Although the reduction potentials of all the REEs are too low (<–2 V vs. SHE) for electrowinning, based on available solubility product data,<sup>42</sup> it is expected that REE hydroxides will precipitate in the range of pH 3–7. ICP-MS analysis of the precipitates collected at pH 9 confirms this hypothesis,

which shows the presence of REEs with a total REE content of  $\sim 70$  mg/kg, with the majority of non-REE species being Al and Fe.

Despite being  $\sim 3.5$  times more concentrated compared with the starting ash, the total REE content in the pH 9 precipitates is still relatively low. However, given other ashes or feedstocks with higher REE content, a 3.5 concentration factor has the potential to produce a valuable REE concentrate. For example, an MSWI ash with >6 mg/kg Sc content would lead to a pH 9 precipitate with >20 mg/kg Sc, which is considered a viable Sc ore.<sup>43</sup> Examples of MSWI ashes with >6 mg/kg Sc content have previously been reported.<sup>15</sup> Thus, although the particular feedstock used in this work does not contain critical materials with concentrations justifying their recovery, these processes can be adapted to feedstocks that do, for example, e-waste or mine tailings, which can contain more than 1,000  $\mu\text{g}/\text{kg}$  of these valuable elements.<sup>13,40</sup>

### Technoeconomic analysis

To be economically viable, the proposed model of using WTE electricity to power an MSWI ash mining process must yield a better return than the current model of selling WTE electricity while incurring ash disposal fees. Here, we first show that the electricity produced by the WTE plant is more than sufficient to power the proposed ash mining process.

Data from York County Solid Waste Authority (YCSWA) shows that this facility processed 466,316 tonnes of MSW in 2022, producing 299 GWh of electricity, 153,000 tonnes of bottom ash, and 27,000 tonnes of fly ash (e.g., 1.83 kWh/kg-ash). 13.7% of the electricity was used for internal operations, leaving the remaining 258 GWh exported to the grid and sold at a price of \$20.4 MM. The cost of transportation was \$9.85/tonne-ash, and the disposal fee was \$30.05/tonne-ash, so the total cost of ash disposal was \$4.1MM for 103,000 tonnes of mixed ash residue. Because YCSWA is close to the landfill site (13 miles) and the on-site Ash Recycling and Processing Facility can sort and recycle all the bottom ash produced, the cost of ash disposal here is much lower than other facilities without an ash recycling process. Including other expenses and trash income at the Authority, the net revenue for YCSWA in 2022 is \$4.8 MM, or \$27/tonne of ash produced.

Let us now compare this revenue to that possible from ash mining. As shown in Figure 2B, the York County, PA MSWI bottom ash used in this work has a total theoretically achievable value of \$240/tonne, while our experiments targeted eight elements with a total value of \$123/tonne-ash. Even in the current unoptimized experiments, the combined value of the recovered Cu, Pb, Zn,  $\text{Mg}(\text{OH})_2$ ,  $\text{Ca}(\text{OH})_2$ , and  $\text{SiO}_2$  is \$60/tonne. This

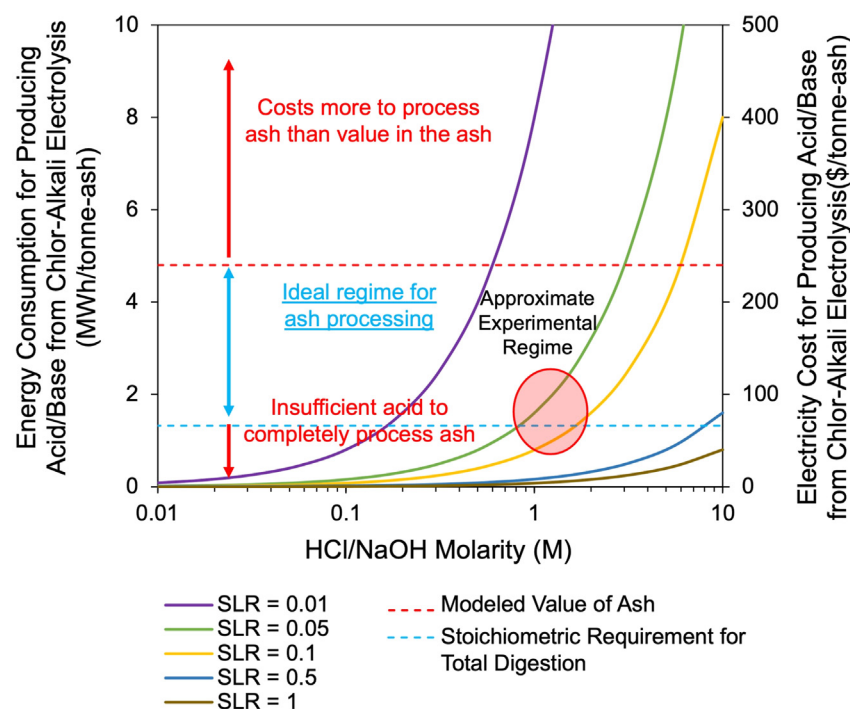


**Figure 5. Technoeconomic analysis wherein WTE electricity is used to power an MSWI ash mining process**

Energy consumption and corresponding electricity cost to produce HCl and NaOH solutions with varying solid-liquid ratios and concentrations using chlor-alkali electrolysis. An electrolyzer efficiency of 2,000 kWh/kg-NaOH. Each curve describes the energy required to produce acid and base sufficient to process a tonne of ash, for a given solid-liquid ratio (SLR) and acid/base molarity. The equivalent electricity cost, assuming an electricity price of \$0.05/kWh is shown on the right-hand axis. The red dashed line represents the calculated ash value (see Figure 2B) of \$240/tonne-ash. The blue dashed line represents the energy consumption (1.3 MWh/tonne-ash) and costs (\$66/tonne-ash) required to produce the stoichiometric minimum of acid and base necessary for complete leaching of all metals, providing the calculated ash value.

number assumes no value for the mixed Fe and Al hydroxides, which, if separated, would increase the total product value to \$90/tonne. This, however, does not include the cost of mining. Here, we estimate the energy consumption and resulting costs for electrolysis and electrowinning. A more detailed technoeconomic analysis appears in a related study.<sup>44</sup>

The primary operating cost (opex) is the electricity cost. The energy consumption and associated electricity cost (assuming \$0.05/kWh) needed to process a tonne of ash using a chlor-alkali reactor to produce the acid and base are plotted in Figure 5. These values are also a function of acid/base concentration and solid-liquid ratio (SLR), as explained in the following paragraph. For a typical chlor-alkali electrolyzer, the specific electricity consumption,  $E_{\text{specific}}$ , is 2,000 kWh/kg-NaOH (2,194 kWh/kg<sub>HCl</sub> = 80 kWh/mol<sub>NaOH</sub> = 80 kWh/mol<sub>HCl</sub>).<sup>27</sup> The number of moles required per tonne of ash digestion is the ratio of the molarity (mol/L) to the SLR (tonne<sub>ash</sub>/L). This quantity can be used to calculate the energy requirement for electrolysis per tonne of ash (kWh/tonne<sub>ash</sub>).

The minimum amount of acid to fully leach the soluble portion of the solid ash can be calculated from the metal concentrations in ash (Equation S5); this acid has an energy and cost represented by the horizontal dashed blue line (1.3 MWh/tonne-ash, \$66/tonne-ash). However, in practice, an excess of acid, described by the SLR (kg/L), is necessary to improve rheology, leaching efficiency, and leaching kinetics.<sup>19,39</sup> In our experiments, we used 1.5–2 times the stoichiometric amount of acid required to dissolve the metals. However, if the cost of producing this acid and base exceeds the maximum value extractable from the ash (horizontal red line, \$240/tonne-ash), then ash mining by the proposed method cannot be net positive in cost (Figure 5). Therefore, for ash min-

ing to be economically viable, the cost of acid and base production must at least lie between the red and blue lines. Although increasing the acid concentration and/or decreasing the SLR improves ash-

leaching kinetics, it also sharply increases the energy consumption and associated cost, creating a tradeoff between lower cost and higher leaching efficiency. Although we did not fully explore this optimization, the experimental regime examined in this work lies toward the lower energy/cost rather than the higher acid concentration regime and requires 1–2 kWh/kg-ash.

In addition to the energy required to produce the reagents, we consider the energy required for materials recovery. For hydroxide precipitation, since the base required is produced concurrently with the acid, no additional electrolysis cost is incurred. For electrowinning, the energy consumption is

$$E_{\text{electrowinning}} = \sum_m \frac{V_m Q_m}{\beta_m} = \sum_m \frac{V_m c_m z_m F}{\beta_m m_m} \quad (\text{Equation 2})$$

where  $m$  is the target metal,  $E_{\text{electrowinning}}$  is the energy per unit mass of ash (kWh/kg-ash),  $V$  is the cell voltage (V) for a given target metal,  $Q_m$  is the amount of metal in charge equivalents of the target metal per unit mass of ash (coulombs/kg-ash),  $\beta$  is the current efficiency (defined as the amount of metal plated, in charge equivalents, relative to the total charge passed) for electrowinning of the target metal,  $z_m$  is the metal ion valence,  $F$  is Faraday's constant,  $m_m$  is the molar mass of metal  $m$ , and  $c_m$  is the concentration of metal  $m$  leached from the ash (g/kg-ash). Based on the experimentally measured cell voltages, current efficiencies, and electrowinning times, for each of Cu, Pb, and Zn, we calculate a total energy consumption for recovery of all three metals to be 0.3 MWh/tonne-ash. Note that even for the present unoptimized experiments, this cost is only 15%–30% of the energy required for electrolysis (1–2 MWh/tonne-ash).

Thus, the energy required for electrolysis and the ensuing leaching and precipitation, and electrowinning, together is  $\sim 2$  kWh/kg-ash. Because the electricity output from typical WTE plant operation (after subtracting the 15% used for internal plant operation) is 2.1 kWh/kg-ash, there appears to be sufficient electricity production to carry out these processes. Because WTE plants are already grid connected, co-location of the materials recovery plant allows easy access to additional electricity. Based on the expected value of the product streams calculated prior (\$90/tonne-ash), up to 41% additional electricity cost (0.82 kWh/kg-ash, at \$0.05/kWh) could be incurred while still generating greater revenue than in the current WTE model of selling electricity (\$49/tonne-ash). Although these calculations only consider the energy consumption of electrolysis and electrowinning, these two unit operations are the most energy intensive. Our current experiments yielded \$60/tonne-ash product value out of a potentially realizable value of \$123/tonne (from the eight target elements). Adding the averted transportation and landfilling costs of \$40/tonne-ash, our experimentally validated return from mining the ash is \$100/tonne-ash. We emphasize here that the avoidance of transportation and landfilling costs is 40% of the total return on this process. Thus, although the individual unit operations are simple and based on industrially practiced processes, the biggest benefit from such a process is the reduction in amount of waste produced. Rather than recovering only a fraction of the material from the waste, decomposing the entirety of the waste into valuable product streams is key to overcoming both the challenges of economical materials recovery and waste management. Improvements in leaching efficiency, which reduces the consumption of acid, and in separation efficiency can further improve this return. However, it is already about two times higher than in the current model of selling MSWI electricity and paying the ash disposal costs. A more detailed analysis<sup>44</sup> that also includes labor, utilities, materials, and capital costs shows that an optimized plant at the scale of 40,000 tonnes-ash/year would be profitable with a net revenue of \$94/tonne-ash. Note that net revenues in the current WTE operating model may well decrease in the future as electricity prices drop and landfilling costs increase.<sup>44</sup> The proposed process is not inherently limited to the mining of MSWI ash and can be tailored toward recovery from other waste streams. Some waste streams of interest include e-waste, which is particularly rich in metals like Cu and Pb; industrial tailings like bauxite residue, which is richer in REEs than the present ash; and mine tailings. This inherent flexibility of an aqueous electrochemistry-based process creates a generalized framework for materials recovery that can be extended to a variety of waste feedstocks.

This work proposes and experimentally validates an electrochemical mining operation that separates MSWI ash into value-added outputs while creating no additional waste streams. Using acids and bases, which may be electrolytically produced using the electricity output of the MSWI plant, acid leaching of the MSWI ash followed by aqueous electrowinning of metals, including Cu, Pb, and Zn, from the leachate is demonstrated. The leachate is subsequently processed by pH-induced precipitation of metal hydroxides, including those of Al, Fe, Mg, and Ca. It is shown that these elements can be selectively recovered at

>90% purity for each of Cu, Pb, Mg, and Ca, and with high recovery efficiencies >80% for all target elements. The energy consumption for the proposed process sequence is quantified, from which it is shown that, firstly, the electricity output of a typical WTE facility is sufficient to power the electrochemical mining operation, and secondly, that the value of the ash mined is about a factor of two greater than the value of the electricity sold, when the avoidance of ash disposal fees is taken into account. Furthermore, by decomposing the entirety of the waste stream into valuable products, the process acts as both a method for materials recovery and a method for waste management. We avoid the  $\sim$ \$50/tonne landfilling fee as well as the pollution from Pb and other heavy metals. The proposed electrochemical process may provide a cost-competitive pathway toward zero-waste urban mining to address future challenges in waste management, mining, and materials supply chains.

## EXPERIMENTAL PROCEDURES

### Resource availability

#### Lead contact

Further information and requests for resources and reagents should be directed to and will be fulfilled by the lead contact, Yet-Ming Chiang ([ychiang@mit.edu](mailto:ychiang@mit.edu)).

#### Materials availability

This study did not generate new, unique reagents.

#### Data and code availability

All data reported in this paper will be shared by the lead contact upon request.

### Materials

The ash used in this work is MSWI bottom ash, collected and supplied by the York County Resource and Recovery Center (York, Pennsylvania, USA) in March 2021 (Figure S3). Prior to receiving, the ash was presorted by the facility into different fractions (Figure S4). The compositions of as-received ash fraction samples are shown in Figure S5. The fraction used in this work is the fine ash fraction collected after magnetic and density separation, wash-screening, and cycloning (Figure S4). This particular fraction was chosen as it contained an optimal combination of particle size (no large pieces of residual MSW) and representative composition (no major elements with outlying concentrations).

### Ash-leaching procedure

Prior to leaching, the ash was roller milled in ethanol for 24 h with ZrO<sub>2</sub> milling media and then dried and passed through a 1 mm sieve. Stock solutions made from HCl (reagent grade HCl 37%, VWR) and Milli-Q UltraPure Water were used for all leaching experiments. Ash leaching was conducted under a variety of HCl acid concentrations with a solid-to-liquid ratio of 0.1 g/mL at room temperature. After ash leaching, the solution was filtered through a 0.2  $\mu$ m polypropylene filter using vacuum filtration. The insoluble material was rinsed with deionized (demineralized or DI) water until the eluent had a pH > 5.

### Electrowinning procedure

After the leaching of the MSWI ash, metals were recovered from the filtered leachates by electrowinning. Electrowinning from the leachate was conducted using glass electrochemical cells maintained at a constant 60°C in a temperature-controlled water bath and stirring at 500 rpm. Two Pt mesh electrodes were used as the working and counter electrodes with an Ag/AgCl reference electrode. Electrowinning was conducted at a constant potential, controlled by a SolarTron 1470E potentiostat, for a fixed duration of time. After electrowinning, the electrodes were removed from the solution and immediately rinsed with DI water. The remaining solution was collected for further experimentation.

### Chemical precipitation procedure

Metal hydroxides were recovered from the filtered leachates through an increase in the solution pH. Solutions made from NaOH pellets (98%, Alfa Aesar) and Milli-Q UltraPure Water were used as reagents for the precipitation of metal hydroxides. Hydroxide precipitation was conducted at room temperature. Although stirring at 500 rpm, the pH was increased through the dropwise addition of NaOH. The pH was constantly monitored using a Sper Scientific pH meter. Once the pH was stable at the desired pH, the solution was filtered using vacuum filtration through a 0.2  $\mu$ m propylene filter. The remaining solution was then collected for further experimentation. The collected precipitates were rinsed with DI water and air-dried for further analysis.

### Compositional analysis of materials and solution using ICP spectroscopy

Compositional analysis of the ash, ash leachates, and the recovered materials was performed using ICP-OES (Agilent ICP-OES 5100 VDV), and ICP-MS (Tandem Triple Quadrupole Mass Spectrometer). The ash leachates were diluted with DI water to an HCl concentration of 5 vol % and then filtered through a 0.2  $\mu$ m polypropylene filter. Similarly, ICP analysis of solid materials was conducted by dissolving the materials in 5 vol % HNO<sub>3</sub> depending on the material and then filtered through a 0.2  $\mu$ m polypropylene filter. The compositions were then analyzed using appropriate standards (Inorganic Ventures). To quantify the concentrations of PGMs and PMs, the solid materials were leached in concentrated aqua regia for 24 h before diluting to a 5 vol % solution and filtering for ICP-MS analysis. Similarly, the REEs were quantified by leaching the solid materials in concentrated HNO<sub>3</sub> before diluting them to a 5 vol % solution and filtering for ICP-MS analysis.

### Materials characterization

The MSWI ash and recovered materials were analyzed using XRD. XRD was performed using a PANalytical X'Pert PRO X-ray diffractometer, and the spectra were analyzed using HighScore+ software. Quantification of the amorphous content in the ash and insoluble residue was determined by mixing the ash with crystalline silicon powder (99.5%, Alfa Aesar) in a 1:1 mass ratio in an agate mortar and pestle. The silicon was used as an internal reference during the XRD. Energy dispersive X-ray spectroscopy (EDS) was also used to determine the major elements in the MSWI ash. EDS was conducted using a Phenom ProX (nanoScience Instruments) scanning electron microscope (SEM).

### SUPPLEMENTAL INFORMATION

Supplemental information can be found online at <https://doi.org/10.1016/j.crsus.2024.100120>.

### ACKNOWLEDGMENTS

This work was funded by the Advanced Research Projects Agency – Energy (ARPA-E) Mining Incinerated Disposal Ash Streams (MIDAS) program under contract DE-AR0001395, Douglas Wicks, Program Director. D.Z. acknowledges the funding provided by ExxonMobil Research and Engineering Company through MIT's Energy Initiative Postdoctoral Fellowship. The authors thank David Vollero, Douglas Jasitt, and Jennifer Cristofolletti from the YCSWA, Anne Hewes, Ph.D., Environmental Manager of ecomaine, and Chris Averyt and Kelle R. Vigeland from the City of Spokane for providing MSWI ash samples and for data on WTE operations. The authors acknowledge Elsa A. Olivetti, Yixi Tian, and Jacqueline Ewuraesi Baidoo of MIT and Angela Noori Son from Harvard Business School for helpful discussions and Charles M. Setters for technical support. This work utilized facilities at MIT.nano and the MIT Institute of Soldier Nanotechnologies.

### AUTHOR CONTRIBUTIONS

Methodology, M.J.W., D.Z., S.C.C.'t.W., and S.Z.; data collection, D.Z., M.J.W., and S.Z.; writing, M.J.W., D.Z., and Y.-M.C.; conceptualization, supervision, and funding acquisition, Y.-M.C.

### DECLARATION OF INTERESTS

Y.-M.C., S.C.C.'t.W., S.Z., and M.J.W. are among inventors on patent applications related to the subject of this manuscript filed by Massachusetts Institute of Technology.

Received: March 11, 2024

Revised: April 21, 2024

Accepted: May 13, 2024

Published: June 5, 2024

### REFERENCES

- US EPA (2017). National overview: facts and figures on materials, wastes and recycling. <https://www.epa.gov/facts-and-figures-about-materials-waste-and-recycling/national-overview-facts-and-figures-materials>.
- US EPA (2016). Frequent questions about landfill gas. <https://www.epa.gov/lmop/frequent-questions-about-landfill-gas>.
- Pierson R., Cross J.-M. Landfill methane. 2013. <https://www.eesi.org/papers/view/fact-sheet-landfill-methane>
- Cho, B.H., Nam, B.H., An, J., and Youn, H. (2020). Municipal solid waste incineration (MSWI) ashes as construction materials—a review. *Materials* (Basel) 13, 3143. <https://doi.org/10.3390/ma13143143>.
- U.S. Energy Information Administration (EIA) (2023). Waste-to-energy plants are a small but stable source of electricity in the United States. <https://www.eia.gov/todayinenergy/detail.php?id=55900>.
- Oehmig, W.N., Roessler, J.G., Blaisi, N.I., and Townsend, T.G. (2015). Contemporary practices and findings essential to the development of effective MSWI ash reuse policy in the United States. *Environ. Sci. Policy* 51, 304–312. <https://doi.org/10.1016/j.envsci.2015.04.024>.
- US EPA (2016). Energy recovery from the combustion of municipal solid waste (MSW). <https://www.epa.gov/smm/energy-recovery-combustion-municipal-solid-waste-msw>.
- Rodricks, N. (2020). Waste into X and the MIDAS touch, advancements in technology can revitalize America's aging waste-to-energy infrastructure. <http://arpa-e.energy.gov/news-and-media/blog-posts/waste-x-and-midas-touch>.
- ACSWMD. Beginner's Guide to Reducing Waste. <https://www.addisoncountyclecycling.org/recycling/reduce-reuse/plastics-reduction>.
- Wagner, T.P., and Raymond, T. (2015). Landfill mining: case study of a successful metals recovery project. *Waste Manag.* 45, 448–457. <https://doi.org/10.1016/j.wasman.2015.06.034>.
- Šyc, M., Simon, F.G., Hykš, J., Braga, R., Biganzoli, L., Costa, G., Funari, V., and Grosso, M. (2020). Metal recovery from incineration bottom ash: state-of-the-art and recent developments. *J. Hazard. Mater.* 393, 122433. <https://doi.org/10.1016/j.jhazmat.2020.122433>.
- Tian, Y., Dai, S., and Wang, J. (2023). Environmental standards and beneficial uses of waste-to-energy (WTE) residues in civil engineering applications. *Waste Dispos. Sustain. Energy* 5, 323–350. <https://doi.org/10.1007/s42768-023-00140-8>.
- Binnemans, K., Jones, P.T., Blanpain, B., Van Gerven, T., and Pontikes, Y. (2015). Towards zero-waste valorisation of rare-earth-containing industrial process residues: a critical review. *J. Cleaner Prod.* 99, 17–38. <https://doi.org/10.1016/j.jclepro.2015.02.089>.
- Allegrini, E., Maresca, A., Olsson, M.E., Holtze, M.S., Boldrin, A., and Astrup, T.F. (2014). Quantification of the resource recovery potential of municipal solid waste incineration bottom ashes. *Waste Manag.* 34, 1627–1636. <https://doi.org/10.1016/j.wasman.2014.05.003>.
- Funari, V., Braga, R., Bokhari, S.N.H., Dinelli, E., and Meisel, T. (2015). Solid residues from Italian municipal solid waste incinerators: A source for “critical” raw materials. *Waste Manag.* 45, 206–216. <https://doi.org/10.1016/j.wasman.2014.11.005>.
- Yao, Q., Samad, N.B., Keller, B., Seah, X.S., Huang, L., and Lau, R. (2014). Mobility of heavy metals and rare earth elements in incineration bottom



- ash through particle size reduction. *Chem. Eng. Sci.* **118**, 214–220. <https://doi.org/10.1016/j.ces.2014.07.013>.
17. Joseph, A.M., Snellings, R., Van den Heede, P., Matthys, S., and De Belie, N. (2018). The use of municipal solid waste incineration ash in various building materials: A Belgian point of view. *Materials (Basel)* **11**, 141. <https://doi.org/10.3390/ma11010141>.
18. Morf, L.S., Gloor, R., Haag, O., Haupt, M., Skutan, S., Di Lorenzo, F.D., and Böni, D. (2013). Precious metals and rare earth elements in municipal solid waste – sources and fate in a Swiss incineration plant. *Waste Manag.* **33**, 634–644. <https://doi.org/10.1016/j.wasman.2012.09.010>.
19. Tang, J., and Steenari, B.-M. (2016). Leaching optimization of municipal solid waste incineration ash for resource recovery: A case study of Cu, Zn, Pb and Cd. *Waste Manag.* **48**, 315–322. <https://doi.org/10.1016/j.wasman.2015.10.003>.
20. Kuboňová, L., Langová, Š., Nowak, B., and Winter, F. (2013). Thermal and hydrometallurgical recovery methods of heavy metals from municipal solid waste fly ash. *Waste Manag.* **33**, 2322–2327. <https://doi.org/10.1016/j.wasman.2013.05.022>.
21. Kalmykova, Y., and Fedje, K.K. (2013). Phosphorus recovery from municipal solid waste incineration fly ash. *Waste Manag.* **33**, 1403–1410. <https://doi.org/10.1016/j.wasman.2013.01.040>.
22. Armstrong, R.D., Todd, M., Atkinson, J.W., and Scott, K. (1996). Selective electrodeposition of metals from simulated waste solutions. *J. Appl. Electrochem.* **26**, 379–384. <https://doi.org/10.1007/BF00251322>.
23. Ajiboye, A.E., Olasehinde, F.E., Adebayo, O.A., Ajayi, O.J., Ghosh, M.K., and Basu, S. (2019). Extraction of copper and zinc from waste printed circuit boards. *Recycling* **4**, 36. <https://doi.org/10.3390/recycling4030036>.
24. Tian, Y., Boursalas, A.C.T., Kawashima, S., and Themelis, N.J. (2023). Using Waste-to-Energy Fine-Combined Ash as Sand or Cement Substitute in Cement Mortar. *J. Mater. Civ. Eng.* **35**, 04023378. <https://doi.org/10.1061/JMCEE7.MTENG-15684>.
25. Ellis, L.D., Badel, A.F., Chiang, M.L., Park, R.J.-Y., and Chiang, Y.-M. (2020). Toward electrochemical synthesis of cement—an electrolyzer-based process for decarbonating CaCO<sub>3</sub> while producing useful gas streams. *Proc. Natl. Acad. Sci. USA* **117**, 12584–12591. <https://doi.org/10.1073/pnas.1821673116>.
26. Paidar, M., Fateev, V., and Bouzek, K. (2016). Membrane electrolysis—history, current status and perspective. *Electrochim. Acta* **209**, 737–756. <https://doi.org/10.1016/j.electacta.2016.05.209>.
27. Kumar, A., Du, F., and Lienhard, J.H. (2021). Caustic soda production, energy efficiency, and electrolyzers. *ACS Energy Lett.* **6**, 3563–3566. <https://doi.org/10.1021/acsenenergylett.1c01827>.
28. Yan, C., Lv, C., Jia, B.-E., Zhong, L., Cao, X., Guo, X., Liu, H., Xu, W., Liu, D., Yang, L., et al. (2022). Reversible Al metal anodes enabled by amorphization for aqueous aluminum batteries. *J. Am. Chem. Soc.* **144**, 11444–11455. <https://doi.org/10.1021/jacs.2c04820>.
29. Hosoya, T., Yonezawa, T., Yamauchi, N., Nakashima, K., and Kobayashi, Y. (2021). Synthesis of metallic aluminum particles by electrolysis in aqueous solution. *Micro Nano Syst. Lett.* **9**, 14. <https://doi.org/10.1186/s40486-021-00141-4>.
30. Satoh, S.. Electrolytic process for the production of metallic titanium from aqueous solution of titanium compounds. <https://patents.google.com/patent/US3074860A/en>.
31. U.S. Geological Survey (2023). Mineral Commodity Summaries 2023. <https://doi.org/10.3133/mcs2023>.
32. Recycling Product News (2023). Breaking down the factors behind scrap glass prices. <https://www.recyclingproductnews.com/article/27088/expert-qanda-breaking-down-the-factors-behind-scrap-glass-prices>.
33. Aber, S. (2023). 2022 MSW Landfill Tipping Fees. Environmental Research & Education Foundation. <https://erefdn.org/2022-msw-landfill-tipping-fees/>.
34. Suraneni, P., and Weiss, J. (2017). Examining the pozzolanicity of supplementary cementitious materials using isothermal calorimetry and thermogravimetric analysis. *Cem. Concr. Compos.* **83**, 273–278. <https://doi.org/10.1016/j.cemconcomp.2017.07.009>.
35. Singh, D., and Kumar, A. (2017). Geo-environmental application of municipal solid waste incinerator ash stabilized with cement. *J. Rock Mech. Geotech. Eng.* **9**, 370–375. <https://doi.org/10.1016/j.jrmge.2016.11.008>.
36. Lam, C.H.K., Barford, J.P., and McKay, G. (2011). Utilization of municipal solid waste incineration ash in Portland cement clinker. *Clean Techn. Environ. Policy* **13**, 607–615. <https://doi.org/10.1007/s10098-011-0367-z>.
37. Fly Ash Price Trend and Forecast (2023). <https://www.chemicalanalyst.com/Pricing-data/fly-ash-1459#:~:text=The%20decrease%20in%20demand%20for,gap%20between%20demand%20and%20supply>.
38. Ferreira, B.K. (2008). Three-dimensional electrodes for the removal of metals from dilute solutions: a review. *Miner. Process. Extr. Metall. Rev.* **29**, 330–371. <https://doi.org/10.1080/08827500802045586>.
39. Vegliò, F., Quaresima, R., Fornari, P., and Ubaldini, S. (2003). Recovery of valuable metals from electronic and galvanic industrial wastes by leaching and electrowinning. *Waste Manag.* **23**, 245–252. [https://doi.org/10.1016/S0956-053X\(02\)00157-5](https://doi.org/10.1016/S0956-053X(02)00157-5).
40. Lister, T.E., Wang, P., and Anderko, A. (2014). Recovery of critical and value metals from mobile electronics enabled by electrochemical processing. *Hydrometallurgy* **149**, 228–237. <https://doi.org/10.1016/j.hydromet.2014.08.011>.
41. Monhemius, A.J. (2017). The iron elephant: A brief history of hydrometallurgists' struggles with element no. 26. In *International Mineral Processing Congress Proceedings*, pp. 1–14. <https://doi.org/10.15834/cimj.2017.21>.
42. W.M. Haynes, ed. (2016). *CRC Handbook of Chemistry and Physics*, Ninety-Seventh Edition (CRC Press), p. 2643. <https://doi.org/10.1201/9781315380476>.
43. Wang, W., Pranolo, Y., and Cheng, C.Y. (2011). Metallurgical processes for scandium recovery from various resources: a review. *Hydrometallurgy* **108**, 100–108. <https://doi.org/10.1016/j.hydromet.2011.03.001>.
44. Baidoo, J., Roth, R., Zhang, D., Wang, M.J., Chiang, Y.-M., and Olivetti, E. (2024). Techno-Economic Assessment of Electrochemical Metals Recovery from Municipal Solid Waste Incineration Ash. <https://ssrn.com/abstract=4798590>.

**CRSUS, Volume 1**

## **Supplemental information**

**Toward zero-waste resource recovery  
from municipal solid waste incineration ash  
by electrochemical and chemical mining**

**Duhan Zhang, Michael J. Wang, Sophie C. Coppieters `t Wallant, Sonia Zhang, and Yet-Ming Chiang**

# Supplemental Information

## **1. Supplemental Characterization**

*1.1 X-ray diffraction of as-received ash and the acid-leached insoluble materials*

*1.2 TGA and characterization of SCM*

## **2. Supplemental Ash Sourcing Information**

## **3. Supplemental Estimation of Separation Condition**

*3.1 Estimation of Reduction Potential for Electrowinning Condition*

*3.2 Estimation of pH for Precipitation Condition*

## **4. Supplemental Technoeconomic Estimation**

## **References**

## 1. Supplemental Characterization

### 1.1 X-ray diffraction of as-received ash and the acid-leached insoluble materials

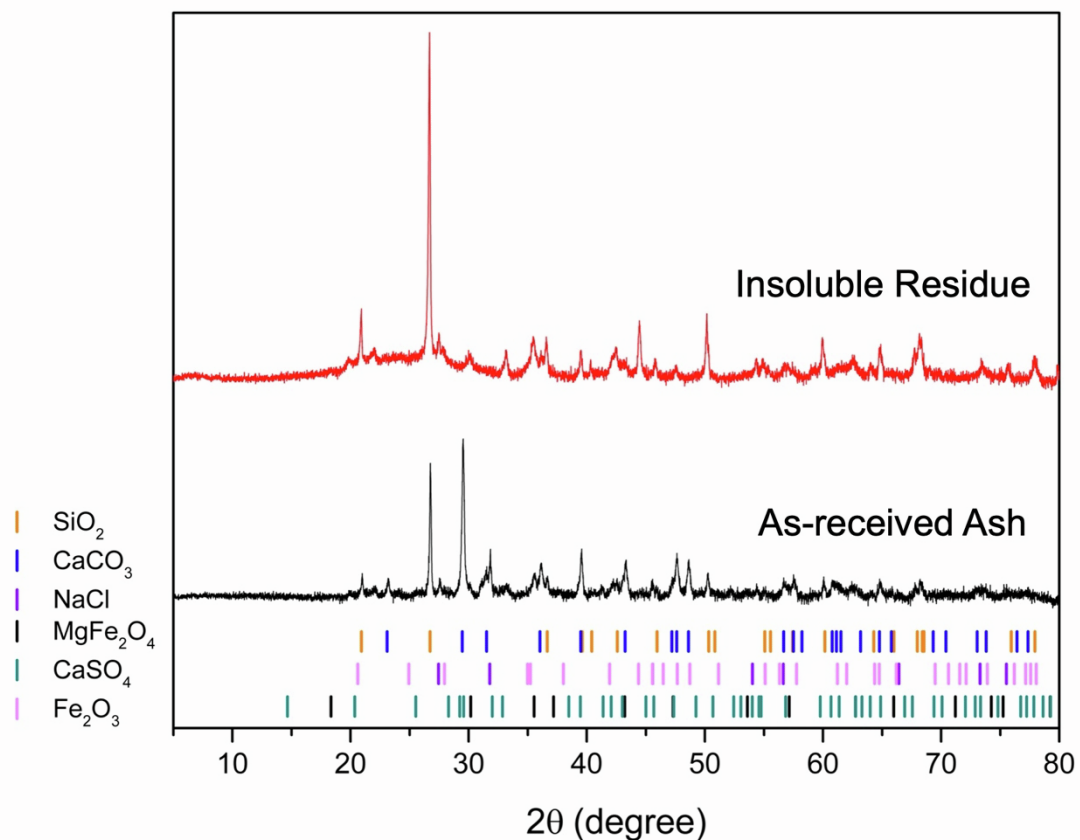


Figure S1. X-ray diffraction (XRD) of as-received ash and the acid-leached insoluble material. The crystalline components of the as-received ash are primarily quartz (SiO<sub>2</sub>) and calcite (CaCO<sub>3</sub>) with minor amounts of the crystalline phases halite (NaCl), magnesioferrite (MgFe<sub>2</sub>O<sub>4</sub>), iron oxide (Fe<sub>2</sub>O<sub>3</sub>), and gypsum (CaSO<sub>4</sub>). The components of acid-leached insoluble residue are mainly quartz phase with small amounts of residual crystalline phases.



### ***Supplemental Note S1. TGA and characterization of SCM***

To characterize the performance of the acid-insoluble ash as supplementary cementitious materials (SCMs), we estimated the pozzolanic reactivity using a thermogravimetric analysis-based approach by Weiss *et al.* [S1]. Test materials were mixed with calcium hydroxide (CH) (CH: SCM = 3:1 by mass) in an alkaline solution (0.5 M KOH; liquid: CH + SCM = 0.9 by mass). 40 g of material was mixed with a spatula for 4 min, and then 7 g of material was transferred in a sealed container and kept in a temperature chamber at 50°C for 10 days. After 10 days, CH consumption was measured using thermogravimetric analysis (TGA, TA Instruments). Approximately 10 mg of the reacted paste was loaded onto a platinum crucible and the measurement was performed by heating from 30°C to 500°C at a rate of 10°C/min in a nitrogen-purged environment. The weight loss around 400°C was used to calculate a CH consumption of 58g of portlandite per 100g of SCM. Based on the pozzolanic activity regimes determined by Weiss *et al.* [S1], a CH consumption of 58g/100g is representative of an SCM with pozzolanic, less reactive material, similar to fly ash and calcined clay.

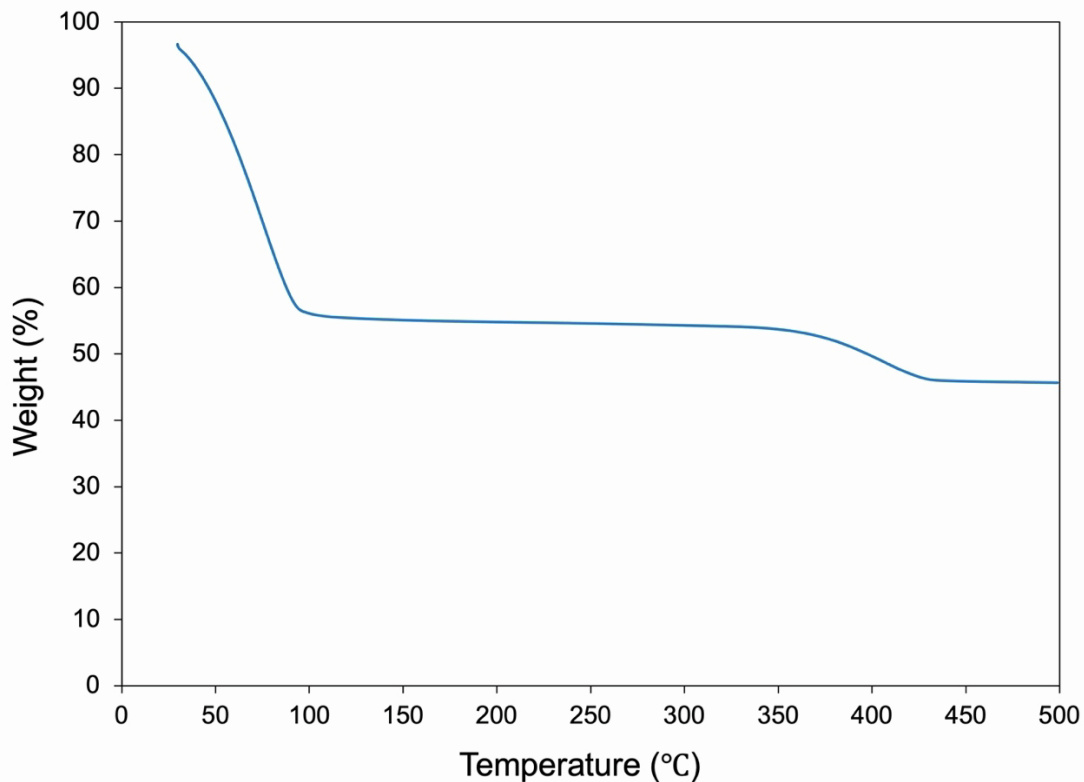


Figure S2. TGA result of ash insoluble, heating from 30°C to 500°C at a rate of 10°C/min in a nitrogen purged environment.

## 2. Supplemental Ash Sourcing Information

**Source:** York County Resource Recovery Center

**Ash Type:** Sorted fly and bottom ash fractions

**Year:** Sampled in March 2021

**Ash Amount:** ~20-30 lbs per fraction

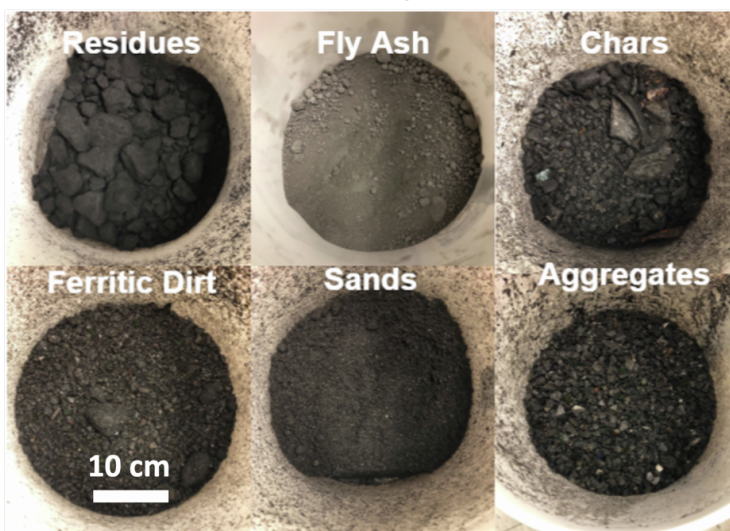


Figure S3. Ash Samples received from York County Resource Recovery Center

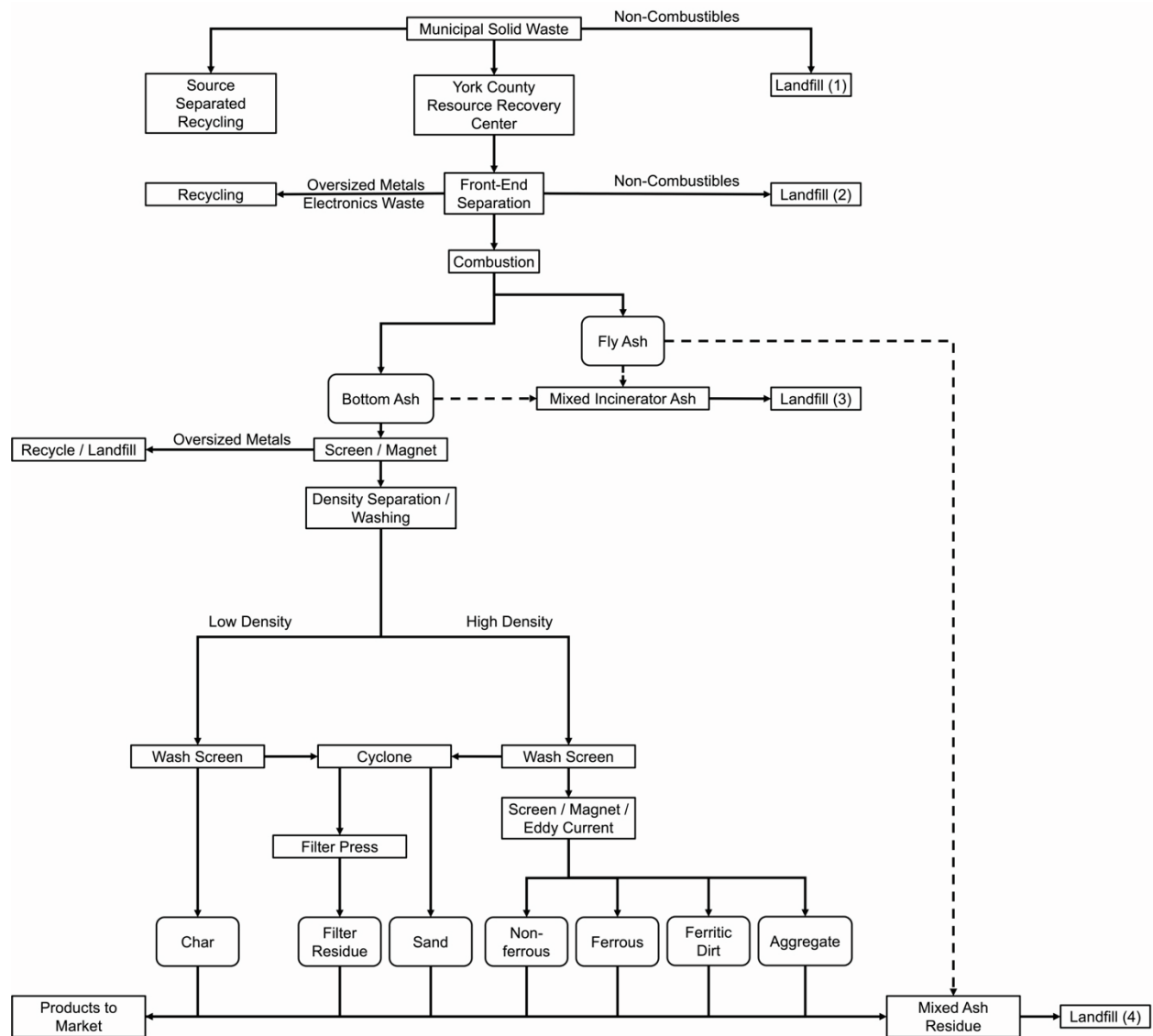


Figure S4. York County Resource Recover Center material flow and ash processing.

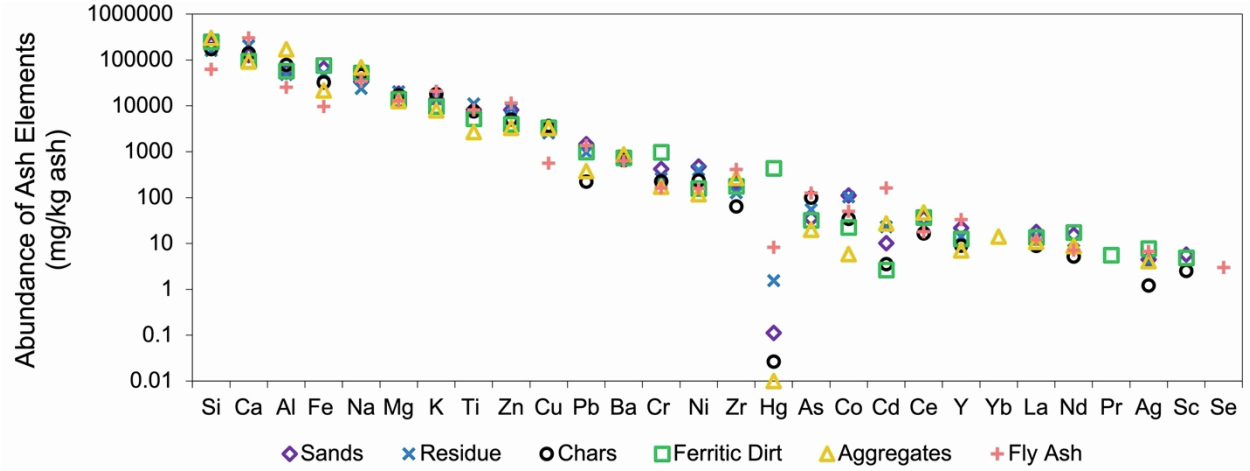


Figure S5. Composition of York County ash fractions measured by ICP, including sand, residue, char, ferritic dirt, aggregate, and fly ash.

### 3. Supplemental Estimation of Separation Condition

#### *Supplemental Note S2. Estimation of Reduction Potential for Electrowinning Condition*

The reduction potential of elements is calculated by the Nernst Equation:

$$M^{n+} + ze^{-} \rightarrow M^0, E^0, \quad (Eq.S1)$$

$$E = E^0 - \frac{RT}{zF} \ln \ln (Q), \quad (Eq.S2)$$

where  $M^{n+}$  is the metal cation,  $E$  is the reduction potential,  $E^0$  is the standard reduction potential,  $R$  is the ideal gas constant,  $T$  is the temperature in Kelvins,  $z$  is the valence,  $F$  is the Faraday constant, and  $Q$  is the reaction quotient.

#### *Supplemental Note S3. Estimation of pH for Precipitation Condition*

The pH at which the metal hydroxide precipitation will occur can be predicted from

$$M(OH)_n \rightarrow M^{n+} + nOH^{-}, K_{sp}, \quad (Eq.S3)$$

$$pH = 14 + \log_{10} \left[ \left( \frac{K_{sp}}{M^{n+}} \right)^{\frac{1}{n}} \right], \quad (Eq.S4)$$

where  $M^{n+}$  is the metal cation,  $K_{sp}$  is the solubility product constant.



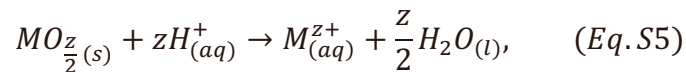
Table S1. Reduction potential and hydroxide solubility constants ( $K_{sp}$ ) for various elements [S2]

Element	Molar Mass (g/mol)	Reduction Potential (V vs SHE)	Hydroxide Solubility Constant ( $K_{sp}$ )	pH of Precipitation (at 0.01M)
Cs	51.996	-2.91		
K	200.59	-2.90		
Li	39.0983	-2.82		
Ca	40.08	-2.86	6.46E-06	11.55
Ba	137.33	-2.81	2.51E-04	13.70
Sr	87.62	-2.79		
Rb	85.4678	-2.66		
Na	54.938	-2.68		
Mg	6.941	-2.33	6.31E-12	8.70
Ce	140.12	-2.24	6.31E-24	7.81
Nd	22.98977	-2.17		
Hf	69.72	-2.13		
Dy	63.546	-2.17		
Sc	44.9559	-1.97	2.22E-31	5.45
P	58.7	-1.74		
Si	28.0855	-1.69		
Al	26.98154	-1.64	3.00E-34	3.04
Zr	91.22	-1.37		
Ti	47.9	-1.31	7.94E-54	1.14
Mn	24.305	-0.99	1.58E-13	8.80
V	50.9415	-1.00		
Zn	65.38	-0.72	6.31E-17	7.07
Cr	251	-0.69	6.70E-31	7.34
Ga	162.5	-0.38	1.00E-37	3.42
Cu	132.9054	-0.29	5.01E-20	5.67
Cd	112.41	-0.24	4.47E-15	9.42
Ni	144.24	-0.21	6.31E-16	8.14
Rh	102.9055	-0.02		
Pb	30.97376	-0.02	1.43E-20	5.26
Sn	118.69	-0.03	5.45E-27	2.82
W	183.85	0.16		
Sb	121.75	0.29		
As	74.9216	0.49		
S	32.06	0.59		
Ag	107.868	0.88	2.00E-08	11.60
Hg	178.49	1.04		

Pd	106.4	1.18		
Pt	195.09	1.43		
Au	196.9665	1.66		

#### Supplemental Note S4. Supplemental Technoeconomic Estimation

To estimate the amount of acid required for complete speciation of all metals in the ash, it was assumed that all metals in the ash exist as a metal oxide. The number of moles of acid, in the form of  $H^+$ , was then calculated based on a generalized form of the metal oxide dissolution reaction in acid:



where  $M$  refers to a given metal with a given valence  $z$ .

Table S2. Assumed costs of elements (USD/tonne) for calculating values of ashes and product streams [S3, S4]. Unless otherwise specified, the cost of each element is taken as a commodity value [S3]. For each element, the element may exist in multiple forms of commodity (i.e. a metal, a metal alloy, an oxide, an ore). The commodity value is a weighted average of the prices of each form of the commodity, weighted by the amount that each form contributes to apparent consumption [S3]. For the elements in which the analysis in this work is more highly sensitive (i.e. Sc, Ti, ...), a specific form of the commodity (i.e. metal, hydroxide, oxide, ore) was chosen based on its likeliest form when recovered from a hydrometallurgical process and the price was updated accordingly. The specific commodity form was also specified for the list of target elements comprising the product streams in this work (Cu, Pb, Zn, Al, Fe, Mg, Ca, Si). The element costs for these elements were chosen in accordance with the form and purity in which they were experimentally recovered.

Element	Cost/tonne	Element	Cost/tonne	Element	Cost/tonne
Rb	\$8,460,548	S	\$93	Ce	\$6,140
Ca (as Ca(OH) <sub>2</sub> )	\$277	Cr	\$2,360	Nb	\$19,700
Fe (as Fe(OH) <sub>2</sub> , bauxite)	\$320	W	\$46,600	Ho	\$129,000
Sc (as Sc <sub>2</sub> O <sub>3</sub> )	\$5,981,962	V	\$16,600	Yb	\$129,000
Na (as NaCl)	\$667	Ta	\$317,000	La	\$6,300
Cu	\$5,960	Co	\$33,100	In	\$615,000
Si (as SiO <sub>2</sub> in fly ash, [S5])	\$75	Pt	\$27,700,000	Lu	\$129,000
Al (as Al(OH) <sub>3</sub> , bauxite)	\$213	Hg	\$30,200	B	\$3,680
Au	\$34,800,000	Dy	\$272,000	Cs	\$50,000
As	\$400,000	Nd	\$63,600	Gd	\$30,900
Mg (as Mg(OH) <sub>2</sub> )	\$648	Pd	\$70,100,000	Ge	\$190,000
K (as KCl)	\$915	Ti (as TiO <sub>2</sub> )	\$60	Cd	\$2,730
Zn	\$2,060	Be	\$660,000	Bi	\$19,200
Rh	\$79,100,000	Y	\$35,500	Sm	\$14,900
Ni	\$12,700	Pr	\$95,500	Se	\$21,400
Sn	\$17,000	Li	\$13,000	Sr	\$79
Ag	\$457,000	Mo	\$26,000	Ir	\$18,300,000
Pb	\$2,000	Tb (as Tb(OH) <sub>4</sub> )	\$640,000	Tm	\$129,000
Zr (as Zr(OH) <sub>2</sub> )	\$16,000	Sb	\$3,900	Tl	\$129,000
Hf	\$830,000	Er	\$129,000	Ru	\$6,370,000
P	\$70	Eu	\$129,000	Te	\$63,500
Mn	\$1,620	Ba	\$180	Ga	\$336

## References

1. Suraneni, P., and Weiss, J. (2017). Examining the pozzolanicity of supplementary cementitious materials using isothermal calorimetry and thermogravimetric analysis. *Cement and Concrete Composites* 83, 273–278.
2. Haynes, W.M. ed. (2016). *CRC Handbook of Chemistry and Physics* 97th ed. (CRC Press) 10.1201/9781315380476.
3. Kelly, T.D., Matos, G.R., Buckingham, D.A., DiFrancesco, C.A., Porter, K.E., Berry, C., Crane, M., Goonan, T., and Sznoppek, J. *Historical Statistics for Mineral and Material Commodities in the United States*. U.S. Geological Survey.  
<https://www.usgs.gov/centers/national-minerals-information-center/historical-statistics-mineral-and-material-commodities>.
4. S&P Global Market Intelligence (2019a). *Mine Economics Methodology*, Market Intelligence Metals & Mining Database. Retrieved from S&P Global.
5. Fly Ash Price Trend and Forecast (2023). <https://www.chemanalyst.com/Pricing-data/fly-ash-1459#:~:text=However%2C%20in%20January%202023%2C%20the,USD%2093%20per%20metric%20ton>.